

Measurement of the Weak Axial-Vector Coupling Constant in the Decay of Free Neutrons Using a Pulsed Cold Neutron Beam

B. Märkisch,^{1,2,*} H. Mest,² H. Saul,^{1,3,4} X. Wang,^{1,3} H. Abele,^{1,2,3,†} D. Dubbers,² M. Klopff,³
A. Petoukhov,⁵ C. Roick,^{1,2} T. Soldner,⁵ and D. Werder²

¹Physik-Department, Technische Universität München, James-Frank-Straße 1, 85748 Garching, Germany

²Physikalisches Institut, Universität Heidelberg, Im Neuenheimer Feld 226, 69120 Heidelberg, Germany

³Technische Universität Wien, Atominstytut, Stadionallee 2, 1020 Wien, Austria

⁴Forschungs-Neutronenquelle Heinz Maier-Leibnitz (FRM II), Technische Universität München, Lichtenbergstraße 1, 85748 Garching, Germany

⁵Institut Laue-Langevin, 71 avenue des Martyrs, CS 20156, 38042 Grenoble Cedex 9, France



(Received 31 January 2019; published 21 June 2019)

We present a precision measurement of the axial-vector coupling constant g_A in the decay of polarized free neutrons. For the first time, a pulsed cold neutron beam was used for this purpose. By this method, leading sources of systematic uncertainty are suppressed. From the electron spectra we obtain $\lambda = g_A/g_V = -1.27641(45)_{\text{stat}}(33)_{\text{sys}}$, which confirms recent measurements with improved precision. This corresponds to a value of the parity violating beta asymmetry parameter of $A_0 = -0.11985(17)_{\text{stat}}(12)_{\text{sys}}$. We discuss implications on the Cabibbo-Kobayashi-Maskawa matrix element V_{ud} and derive a limit on left-handed tensor interaction.

DOI: [10.1103/PhysRevLett.122.242501](https://doi.org/10.1103/PhysRevLett.122.242501)

Measurements in muon and neutron decay link weak leptonic and semileptonic decays to the underlying Lagrangian of the standard model with coupling constants based on the $SU(3)_c \times SU(2)_L \times U(1)$ gauge structure [1–3]. The Fermi coupling constant G_F measured in muon decay [4] provides a low energy value for the weak coupling and was historically used to predict the masses of the W and Z bosons [5–7]. The Lagrange density in semileptonic neutron decay includes a hadronic vector (V) and an axial-vector current (A). The vector coupling constant for quarks g_V is related to that for leptons via $g_V = G_F V_{ud}$, with the matrix element V_{ud} of the Cabibbo-Kobayashi-Maskawa (CKM) quark mixing matrix. The axial-vector current is renormalized by the strong interaction at low energy. This is quantified by the parameter $\lambda = g_A/g_V$, the ratio of the axial-vector and vector coupling constants. If the weak interaction is invariant under time reversal, the parameter λ is real. Using lattice QCD, g_A can be computed with a precision of 1% [8].

The most precise experimental determination of the parameter λ is from the beta asymmetry in neutron decay, but older experimental results [9–11] are not consistent with newer experiments [12,13] with smaller systematic corrections. This discrepancy prevails since the first result of PERKEO II [14] and one aim of this Letter is to clarify the situation.

The ratio of coupling constants λ is important in many fields [15]: it enters in the prediction for the energy consumption in the Sun via the primary reaction in the pp chain and the solar neutrino flux, the production of light elements in primordial nucleosynthesis, and neutron star

formation. λ is also used for the calibration of neutrino detectors and as an input for the unitarity check of the quark-mixing CKM matrix. Within the standard model, the CKM matrix is unitary, and unitarity tests are sensitive tools for searches for new physics [16]. Experimentally, unitarity can be tested with 10^{-4} sensitivity for the first row of the matrix using nuclear decays [17,18], but new results on the universal radiative corrections have raised tension [19,20]. The possible observation of nonstandard model couplings is another example of how new physics could emerge and is typically tested in the framework of effective field theories; for recent reviews and surveys see [8,15,21–25].

In neutron decay, the probability that an electron is emitted with angle ϑ with respect to the neutron spin polarization vector $\mathbf{P} = \langle \boldsymbol{\sigma} \rangle / \sigma$ is [26]

$$W(\vartheta) = 1 + \frac{v}{c} PA \cos \vartheta, \quad (1)$$

where v is the electron velocity. A is the parity violating beta asymmetry parameter, which depends on λ .

In this Letter, we present the first determination of λ from a measurement of the beta asymmetry using a pulsed neutron beam. The method is described in Refs. [27,28] and effectively eliminates or controls leading sources of systematic uncertainty: beam related background, edge effects [29], and the magnetic mirror effect. Yet, one order of magnitude more data was collected compared to the previously most precise experiment [12]. In order to ensure a *blind* analysis, the beta decay data and two major systematic corrections (neutron beam polarization and

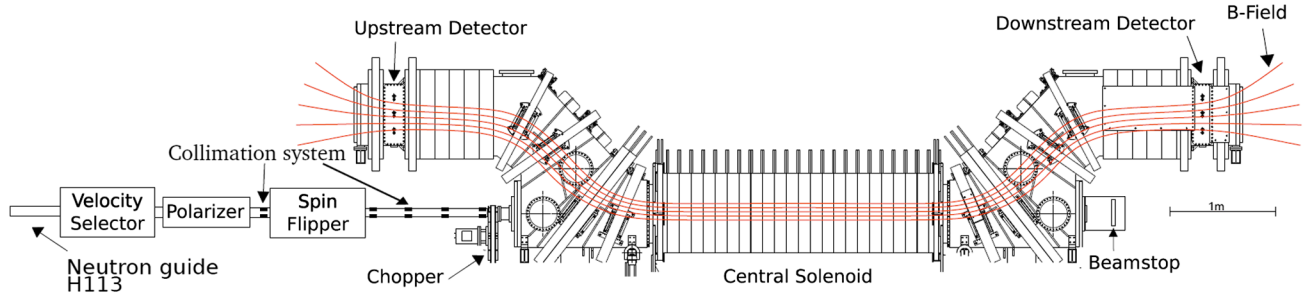


FIG. 1. Schematic of the spectrometer setup PERKEO III installed at PF1B. The magnetic field is indicated in red. The cold neutron beam from the reactor source enters the beam line on the left-hand side. Picture from [35].

magnetic mirror effect) were analyzed separately by independent teams. Results were combined once the analyses were complete.

The spectrometer PERKEO III [27,28] is the successor to the spectrometer PERKEO II, which was used to measure the beta asymmetry parameter A [12,14,30], the neutrino asymmetry parameter B [31,32], and the proton asymmetry parameter C [33] in polarized neutron beta decay. The main component of the spectrometer is an 8 m long magnet system, consisting of 54 short conventional coils with rectangular cross section. The shape of the magnetic field and the beam line setup are shown in Fig. 1. Electrons from neutron decay in the (nearly) homogeneous field in the center of the spectrometer are separated from the neutron beam and guided to two detectors installed upstream and downstream. By using a pulsed beam, neutrons are temporarily stored in flight, fully contained in the decay volume without any contact to material. The solid angle coverage of the detectors is thus truly $2 \times 2\pi$, without edge effects. The magnetic field has its maximum of $B_{\max} = 152.5$ mT in the center of the active region. The field decreases towards the detectors to reduce backscatter effects from the detectors. Details on electron backscatter suppression can be found in Refs. [14,30,34].

The spectrometer was installed at the PF1B cold neutron beam position at the Institut Laue-Langevin [36,37]. Neutrons moderated by a cold source are transported to the beam site via a supermirror guide. The capture flux density measured at the guide's exit was $\Phi = 2 \times 10^{10} \text{ s}^{-1} \text{ cm}^{-2}$. A Dornier neutron velocity selector [38] allowed only neutrons within a wavelength band of 4.5 to 5 Å to enter the instrument's beam line. The neutron beam was subsequently polarized by a single supermirror (SM) coated bender polarizer [39]. The adjustment of the polarizer was optimized for transmission, which also yields a rather symmetrical beam intensity and polarization. An adiabatic fast passage flipper allowed us to reverse the neutron spin direction. A series of five apertures made out of ${}^6\text{LiF}$ were used to shape the neutron beam. Before the neutron beam entered the PERKEO III spectrometer, a rotating disk chopper with a maximum frequency of 6000 rpm was used to pulse the beam as described in Ref. [27]. ${}^6\text{LiF}$

ceramics embedded in the chopper disk made of fiber reinforced plastic were used to absorb the neutron beam. The geometrical opening of the chopper disk was 7.3%. After passing the spectrometer, remaining neutrons were dumped in a ${}^{10}\text{B}_4\text{C}$ beamstop. Data from neutron decay were taken at two different frequencies of the chopper, 83 and 94 Hz. Both datasets have similar sizes. The number of detected decay events as a function of time after the chopper opens is shown in Fig. 2.

When used with a polarized continuous neutron beam, PERKEO III can detect up to 5×10^4 decay events/s [27]. In the current setup—using a pulsed neutron beam—the instantaneous decay rate was reduced to $2 \times 10^3 \text{ s}^{-1}$ during the signal time interval and $1.4 \times 10^2 \text{ s}^{-1}$ on time average. In total, 6×10^8 neutron decay events were used for the extraction of the results.

The polarization of the neutron beam was measured for several rotational speeds of the velocity selector using opaque ${}^3\text{He}$ spin filter cells. Regular *in situ* flipping of the ${}^3\text{He}$ spins served to separate neutron flipping efficiency and polarization. Flat and parallel neutron entrance and exit windows of the filter cells and homogeneous neutron detectors assured a correct spatial averaging over the rectangular aperture used to define the sensitive area.

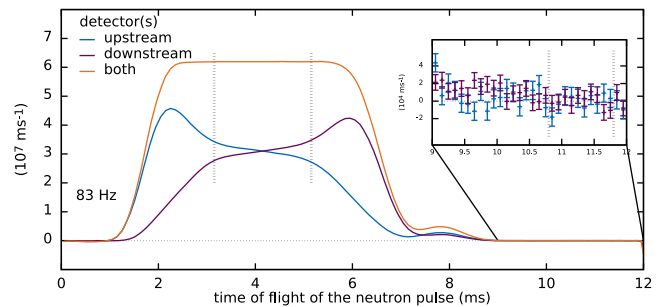


FIG. 2. Number of decay events in the electron energy window 300 to 700 keV as a function of time of flight of the neutron pulse through the spectrometer for a chopper frequency of 83 Hz. Background is subtracted. The shape of the curves for the detectors is caused by the magnetic mirror effect. The vertical lines indicate the time windows used for signal and background extraction. (Inset) Enlargement of the background time window.

The beam-averaged polarization was determined from polarization and intensity scans with step sizes equal to the dimensions of this aperture, avoiding interpolation uncertainties. Scans performed from a shifted reference point yielded consistent results. The derived systematic uncertainty of spatial averaging of 3.4×10^{-4} is dominated by the limited statistical precision of these tests. Measurements in front and behind the PERKEO III spectrometer gave consistent results. Later measurements behind the spectrometer, in between and after the beta decay runs, were used to derive the limit of 3.9×10^{-4} on a potential time variation of the beam polarization. The third leading systematic uncertainty stems from the measured correction for neutron depolarization by the spectrometer exit window of $2.7(2.2) \times 10^{-4}$. The background was determined from regions outside the neutron pulse in the time-of-flight spectra and results in a correction of $2.3(9) \times 10^{-4}$. All other individual corrections and uncertainties, including that for the averaging over the wavelength band, are below 1×10^{-4} . The resulting average neutron polarization of the pulses at the reference selector speed is $P = 0.99100(60)$ and the flipping efficiency is >0.99964 (68.3% C.L.). The combined error of these two effects on the asymmetry is 6.4×10^{-4} . Since we do not use two SM bender polarizers in crossed (X-SM) geometry [40], the resulting neutron polarization is lower than in Ref. [12], but the accuracy is improved by about a factor of 2 due to the limited wavelength band and improved systematic uncertainties [41–44].

Electrons were detected using two plastic scintillators of size $43 \times 45 \text{ cm}^2$, which were each read out by six fine mesh photomultiplier tubes. Monoenergetic conversion electron sources (^{139}Ce , ^{113}Sn , ^{137}Cs , and ^{207}Bi) were used to calibrate and characterize the detectors. The sources were supported by thin carbon foil backings ($<20 \mu\text{g}/\text{cm}^2$) and could be moved in two dimensions across the cross section of the neutron beam in the decay volume. Detector drifts were checked and accounted for with a single source every hour. Twice a day, a full calibration with all sources was performed. The nonlinearity of the detector systems was determined using the calibration sources and off-line measurements of the electronics and the scintillator. While calibration with sources works very well at energies larger than 200 keV, future measurements will also employ a time-of-flight technique to improve calibration at low energies [45,46].

The uniformity of the detectors was measured about once per week. As a major improvement over previous PERKEO measurements, the variation of the detector amplitude over the area covered by decay electrons was $<\pm 2.5\%$. The effect of the detector nonuniformity on our result is dominated by the dependence of the magnetic point-spread function on the beta asymmetry [29,47] and the difference in detector coverage of beta asymmetry and calibration measurements. After unblinding, we corrected

the geometrical coverage of the detector using a previously unapplied analysis, which shifted the result by less than 10% of the final total uncertainty. The corresponding corrections are calculated using photon transport simulations performed with GEANT4 [48]. The resulting detector model fits the measured uniformity under consideration of the electron point spread. The overall nonuniformity correction also includes the effect of energy loss in the carbon foil backings, which only needs to be considered for calibration measurements.

Despite the suppression of backscattering from the detectors by the magnetic field, about 6% of the electrons are reflected onto the opposite detector. Full energy reconstruction is possible, as both detectors are always read out simultaneously. If the deposited energy during the first incidence is not sufficient for a trigger, the wrong emission direction would be assigned to the event. The correction for this effect is calculated based on Monte Carlo backscattering simulations using GEANT4, which have been verified using measured backscattering data [34].

Neutron decay data were only taken while the neutron pulse was fully contained in the homogeneous part of the magnetic field and the chopper was closed. Background was measured at the end of every chopper cycle when the neutron beam had been fully absorbed by the neutron beam dump, see Fig. 2. Signal and background are thus measured under the same condition, i.e., with the chopper closed. The signal-to-background ratio in the fit region was better than 4:1. The time dependence of the ambient background and that created by the closed chopper was checked using ^3He neutron counter tubes, NaI γ detectors, and the PERKEO detector systems. Effects were found to be smaller than $\Delta A/A = 2 \times 10^{-4}$. In previous experiments [12], a significant amount of data had to be discarded due to the variation of background from external sources like neighboring instruments. In this experiment, these sources were tracked without significant delay. The uncertainty on the background measurement was reduced by more than an order of magnitude. The two datasets with different chopper frequencies were used to investigate a possible beam-dependent background.

Electrons are reflected on an increasing magnetic field if the opening angle of gyration with respect to the magnetic field exceeds the critical angle $\theta_c = \arcsin \sqrt{B_1/B_0}$, where B_0 is the maximum of the magnetic field and B_1 is the field at the place of the neutron decay. This modifies the solid angle coverage of the two detectors and hence changes the measured asymmetry. This expected “mirror effect” is calculated from measurements of the shape of the neutron cloud in space and time and magnetic field distributions. The field in the active region was measured with Hall probes on a $3 \times 3 \times 27$ grid with a spacing of 10 cm. Measurements were performed before and after the neutron decay measurements and with different sensors and yield consistent results. The neutron pulse shape in space and

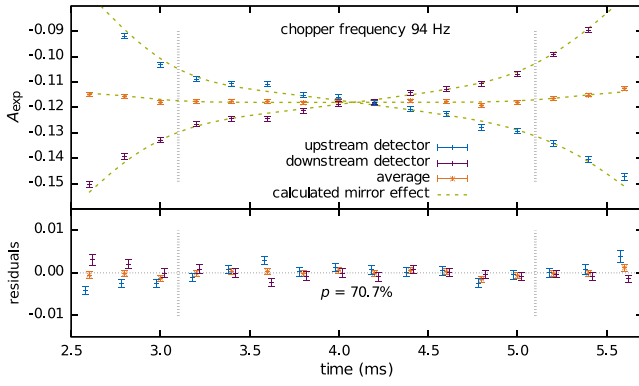


FIG. 3. Measured asymmetry A_{exp} for both detectors as a function of time of flight of the neutron pulse. When averaging over both detectors, the dominant effect of the magnetic mirror effect cancels and only a small correction remains, see Table I. The vertical dashed lines indicate the time window used for the asymmetry analysis, and the curves indicate the calculated mirror effect.

time was measured at several positions downstream of the chopper using different detection techniques [(n, γ) reactions in aluminum foils or absorption in boron and gamma detectors, copper foil activation, and scanning with neutron detectors]. Results are consistent with each other and agree with calculations and McStas [49,50] simulations based on the geometrical properties of selector and chopper. Most of the mirror effect on the asymmetry A cancels by averaging the results of the upstream and downstream detectors, which can be seen in Fig. 3. The remaining average correction of both detectors on the time-averaged asymmetry is $(49.7 \pm 4.5) \times 10^{-4}$ for the 83 Hz and $(42.5 \pm 4.5) \times 10^{-4}$ for the 94 Hz chopper frequencies. We note that this correction is independent of the electron energy.

The electron spectra for both spin states and detectors [$N_i^{\uparrow\downarrow}(E)$, $i = 1, 2$] were used to obtain the experimental asymmetry, which is directly related to the asymmetry parameter A of Eq. (1). Omitting some further correction terms, we obtain

$$A_{\text{exp},i}(E) = \frac{N_i^{\uparrow}(E) - N_i^{\downarrow}(E)}{N_i^{\uparrow}(E) + N_i^{\downarrow}(E)} = \frac{1}{2} \frac{v}{c} AP \frac{M}{1 \pm k}, \quad (2)$$

where the factor $\langle \cos \theta \rangle = 1/2$ results from solid angle integration of Eq. (1). The neutron polarization P , the magnetic mirror correction $M/(1 \pm k)$ [51], and the beta decay data were all analyzed by independent teams.

The asymmetry parameter A includes order 1% corrections for weak magnetism, $g_V - g_A$ interference, and nucleon recoil [52]. For λ real, the uncorrected asymmetry A_0 is given by

$$A_0 = -2 \frac{\lambda(\lambda + 1)}{1 + 3\lambda^2}. \quad (3)$$

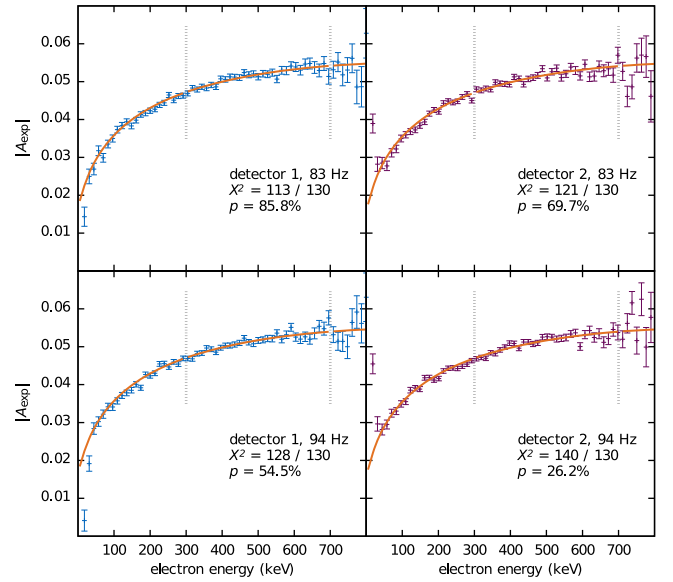


FIG. 4. The experimental asymmetry $|A_{\text{exp},i}(E_e)|$ and fits with a single free parameter λ for both detectors and both chopper frequencies. The solid part of the line indicates the fit interval that was chosen to balance statistics and effects due to detector nonlinearity and unrecognized backscattering.

An additional small radiative correction [53–55] of order 0.1% must be applied.

Figure 4 shows fits to the experimental asymmetry of the available four datasets with the ratio of coupling constants λ as a single free parameter. We note that the calibrations of the detectors were obtained using calibration sources only instead of relying on electron spectra from neutron beta decay. The result is independent of the choice of the fit range within the statistical error. The fit range of about 300 to 700 keV was chosen in order to optimize the combined systematic and statistical uncertainties.

We apply remaining corrections listed in Table I and obtain the final result

$$\begin{aligned} \lambda &= -1.27641(45)_{\text{stat}}(33)_{\text{sys}} \\ &= -1.27641(56), \\ A &= -0.11985(17)_{\text{stat}}(12)_{\text{sys}} \\ &= -0.11985(21). \end{aligned} \quad (4)$$

The result of this blinded analysis confirms recent measurements using cold and ultracold neutrons [12,13] with 2.5 times higher precision compared to [12]. We note that all recent measurements have much smaller corrections on the percent level only compared to older measurements, see also [15].

This result [Eq. (4)] puts severe constraints on exotic decay channels as an explanation of the neutron lifetime anomaly [56].

TABLE I. Summary of corrections to the measured experimental asymmetry and uncertainties. All quantities are given as fractions $\Delta A/A$ of the asymmetry parameter. The fit parameter actually is λ , but we list corrections on A for comparability with earlier measurements.

Effect on asymmetry A	Relative correction (10^{-4})	Relative uncertainty (10^{-4})
Neutron beam		
Polarization and Spin-flip efficiency	90.7	6.4
Background		
Time variation	-0.8	0.8
Chopper	-1.9	0.7
Electrons		
Magnetic mirror effect	46.1	4.5
Undetected backscattering	5.0	1.5
Lost backscatter energy	0	1.4
Electron detector		
Dead time	(5) ^a	0.35
Temporal stability		3.7
Nonuniformity	4.2	2.1
Nonlinearity	(-1) ^a	4
Calibration (input data)		1
Theory		
Radiative corrections	(-10) ^a	1
Total systematics	138.1	10.3
Statistical uncertainty		14.0
<i>Total</i>		17.4

^aAlready included in the fit results shown in Fig. 4: measured by the data acquisition system or included in the fit function.

The transition amplitude V_{ud} of the CKM matrix [57,58] can be derived with our result (4) and the neutron lifetime (6) as input and using Eq. (3) from [20],

$$\begin{aligned}
 V_{ud} &= \left(\frac{5099.34 \text{ s}}{\tau_n(1 + 3\lambda^2)(1 + \Delta_R)} \right)^{1/2} \\
 &= 0.97301(10)_{\text{RC}}(44)_{\tau_n}(35)_{\lambda} \\
 &= 0.97301(58), \tag{5}
 \end{aligned}$$

where Δ_R includes both outer and universal radiative corrections (RCs) and we use the value from [20]. Following Particle Data Group procedures, we update the world average of the neutron lifetime measurements to include new measurements [59–61],

$$\tau_n = 879.7(8) \text{ s.} \tag{6}$$

The neutron result Eq. (5) is in agreement with the average result from superallowed beta decays of $V_{ud} = 0.97395(23)$ [20], Eq. (4), and only 2.5 times less precise, see also [56]. For comparison with earlier results, we note that the universal radiative corrections have significantly

changed recently and also nuclear corrections are being addressed [19,20]. Using the radiative corrections from [62,63] instead, we obtain $V_{ud} = 0.97351(60)$.

As a first application of our result to searches for new physics, we derive an improved limit on hypothetical left-handed tensor interaction. Following the scheme of [64,65] and using our result of the beta asymmetry (4), our average of the neutron lifetime (6), the average nuclear $\mathcal{F}t$ value [20], and the limit on scalar interaction from [17], we obtain

$$-0.0048 < C_T/C_A < 0.0007, \quad (95\% \text{ C.L.}). \tag{7}$$

The authors acknowledge the excellent support of the services of the Physikalisches Institut, Heidelberg University, and the ILL. We thank D. Rechten, TUM, for providing us with ultrathin carbon foils, and U. Schmidt, Heidelberg, for countless valuable discussions. This work was supported by the Priority Programme SPP 1491 of the German Research Foundation (DFG), Contracts No. MA 4944/1-2, No. AB 128/5-2, No. SO 1058/1-1, the Austrian Science Fund (FWF) Contract No. P 26636-N20, the German Federal Ministry for Research and Education, Contracts No. 06HD153I and No. 06HD187, and the DFG cluster of excellence ‘‘Origin and Structure of the Universe’’. The computational results presented have been achieved in part using the Vienna Scientific Cluster (VSC).

*maerkisch@ph.tum.de

†abele@ati.ac.at

- [1] S. L. Glashow, Partial-symmetries of weak interactions, *Nucl. Phys.* **22**, 579 (1961).
- [2] S. Weinberg, A Model of Leptons, *Phys. Rev. Lett.* **19**, 1264 (1967).
- [3] A. Salam, Weak and electromagnetic interactions, *eConf. C680519*, 367 (1968).
- [4] D. M. Webber *et al.* (MuLan Collaboration), Measurement of the Positive Muon Lifetime and Determination of the Fermi Constant to Part-per-Million Precision, *Phys. Rev. Lett.* **106**, 041803 (2011).
- [5] A. Sirlin, Radiative corrections in the $SU(2)_L \times U(1)$ theory: A simple renormalization framework, *Phys. Rev. D* **22**, 971 (1980).
- [6] W. J. Marciano and A. Sirlin, Radiative corrections to neutrino-induced neutral-current phenomena in the $SU(2)_L \times U(1)$ theory, *Phys. Rev. D* **22**, 2695 (1980).
- [7] C. H. Llewellyn Smith and J. F. Wheeler, Electroweak radiative corrections and the value of $\sin^2\theta_w$, *Phys. Lett.* **105B**, 486 (1981).
- [8] C. C. Chang, A. N. Nicholson, E. Rinaldi, E. Berkowitz, N. Garron, D. A. Brantley, H. Monge-Camacho, C. J. Monahan, C. Bouchard, M. A. Clark, B. Joó, T. Kurth, K. Orginos, P. Vranas, and A. Walker-Loud, A per-cent-level determination of the nucleon axial coupling from quantum chromodynamics, *Nature (London)* **558**, 91 (2018).
- [9] P. Bopp, D. Dubbers, L. Hornig, E. Klemt, J. Last, H. Schütze, S. J. Freedman, and O. Schärpf, Beta-Decay

- Asymmetry of the Neutron and g_A/g_V , *Phys. Rev. Lett.* **56**, 919 (1986).
- [10] B. Yerozolimsky, I. Kuznetsov, Y. Mostovoy, and I. Stepanenko, Corrigendum: Corrected value of the beta-emission asymmetry in the decay of polarized neutrons measured in 1990, *Phys. Lett. B* **412**, 240 (1997).
- [11] P. Liaud, K. Schreckenbach, R. Kossakowski, H. Nastoll, A. Bussi ere, J. Guillaud, and L. Beck, The measurement of the beta asymmetry in the decay of polarized neutrons, *Nucl. Phys. A* **612**, 53 (1997).
- [12] D. Mund, B. M arkisch, M. Deissenroth, J. Krempel, M. Schumann, H. Abele, A. Petoukhov, and T. Soldner, Determination of the Weak Axial Vector Coupling $\lambda = g_A/g_V$ from a Measurement of the β -Asymmetry Parameter A in Neutron Beta Decay, *Phys. Rev. Lett.* **110**, 172502 (2013).
- [13] M. A.-P. Brown *et al.* (UCNA Collaboration), New result for the neutron β -asymmetry parameter A_0 from UCNA, *Phys. Rev. C* **97**, 035505 (2018).
- [14] H. Abele, S. Bae ler, D. Dubbers, C. Metz, T. M uller, V. Nesvizhevsky, C. Raven, O. Sch arpf, and O. Zimmer, A measurement of the beta asymmetry A in the decay of free neutrons, *Phys. Lett. B* **407**, 212 (1997).
- [15] D. Dubbers and M. G. Schmidt, The neutron and its role in cosmology and particle physics, *Rev. Mod. Phys.* **83**, 1111 (2011).
- [16] V. Cirigliano, J. P. Jenkins, and M. Gonz alez-Alonso, Semileptonic decays of light quarks beyond the standard model, *Nucl. Phys. B* **830**, 95 (2010).
- [17] J. C. Hardy and I. S. Towner, Superaligned $0^+ \rightarrow 0^+$ nuclear β decays: 2014 critical survey, with precise results for V_{ud} and CKM unitarity, *Phys. Rev. C* **91**, 025501 (2015).
- [18] J. C. Hardy and I. S. Towner, $|V_{ud}|$ from nuclear β decays, *Proc. Sci., CKM2016* (2016) 028.
- [19] C.-Y. Seng, M. Gorchtein, H. H. Patel, and M. J. Ramsey-Musolf, Reduced Hadronic Uncertainty in the Determination of V_{ud} , *Phys. Rev. Lett.* **121**, 241804 (2018).
- [20] C. Y. Seng, M. Gorchtein, and M. J. Ramsey-Musolf, Dispersive evaluation of the inner radiative correction in neutron and nuclear β -decay, [arXiv:1812.03352v2](https://arxiv.org/abs/1812.03352v2).
- [21] M. Gonz alez-Alonso, O. Naviliat-Cuncic, and N. Severijns, New physics searches in nuclear and neutron β decay, *Prog. Part. Nucl. Phys.* **104**, 165 (2019).
- [22] B. R. Holstein, Precision frontier in semileptonic weak interactions: introduction and overview, *J. Phys. G* **41**, 110301 (2014).
- [23] T. Bhattacharya, V. Cirigliano, S. D. Cohen, A. Filipuzzi, M. Gonz alez-Alonso, M. L. Graesser, R. Gupta, and H.-W. Lin, Probing novel scalar and tensor interactions from (ultra)cold neutrons to the LHC, *Phys. Rev. D* **85**, 054512 (2012).
- [24] V. Cirigliano, S. Gardner, and B. R. Holstein, Beta decays and non-standard interactions in the LHC era, *Prog. Part. Nucl. Phys.* **71**, 93 (2013).
- [25] K. K. Vos, H. W. Wilschut, and R. G. E. Timmermans, Symmetry violations in nuclear and neutron β decay, *Rev. Mod. Phys.* **87**, 1483 (2015).
- [26] J. D. Jackson, S. B. Treiman, and H. W. Wyld, Possible tests of time reversal invariance in beta decay, *Phys. Rev.* **106**, 517 (1957).
- [27] B. M arkisch, H. Abele, D. Dubbers, F. Friedl, A. Kaplan, H. Mest, M. Schumann, T. Soldner, and D. Wilkin, The new neutron decay spectrometer PERKEO III, *Nucl. Instrum. Methods Phys. Res., Sect. A* **611**, 216 (2009).
- [28] B. M arkisch, Systematic advantages of pulsed beams for measurements of correlation coefficients in neutron decay, *Phys. Procedia* **51**, 41 (2014).
- [29] D. Dubbers, L. Raffelt, B. M arkisch, F. Friedl, and H. Abele, The point spread function of electrons in a magnetic field, and the decay of the free neutron, *Nucl. Instrum. Methods Phys. Res., Sect. A* **763**, 112 (2014).
- [30] H. Abele, M. Astruc Hoffmann, S. Baessler, D. Dubbers, F. Gl uck, U. M uller, V. Nesvizhevsky, J. Reich, and O. Zimmer, Is the Unitarity of the Quark-Mixing CKM Matrix Violated in Neutron β -Decay? *Phys. Rev. Lett.* **88**, 211801 (2002).
- [31] M. Kreuz, T. Soldner, S. Bae ler, B. Brand, F. Gl uck, U. Mayer, D. Mund, V. Nesvizhevsky, A. Petoukhov, C. Plonka, J. Reich, C. Vogel, and H. Abele, A measurement of the antineutrino asymmetry B in free neutron decay, *Phys. Lett. B* **619**, 263 (2005).
- [32] M. Schumann, T. Soldner, M. Deissenroth, F. Gl uck, J. Krempel, M. Kreuz, B. M arkisch, D. Mund, A. Petoukhov, and H. Abele, Measurement of the neutrino asymmetry parameter B in neutron decay, *Phys. Rev. Lett.* **99**, 191803 (2007).
- [33] M. Schumann, M. Kreuz, M. Deissenroth, F. Gl uck, J. Krempel, B. M arkisch, D. Mund, A. Petoukhov, T. Soldner, and H. Abele, Measurement of the Proton Asymmetry Parameter in Neutron Beta Decay, *Phys. Rev. Lett.* **100**, 151801 (2008).
- [34] C. Roick, H. Saul, H. Abele, and B. M arkisch, Undetected electron backscattering in PERKEO III, [arXiv:1905.10189](https://arxiv.org/abs/1905.10189).
- [35] H. Mest, Ph.D. thesis, Universit at Heidelberg, 2011, <http://www.ub.uni-heidelberg.de/archiv/12198>.
- [36] H. H ase, A. Kn opfler, K. Fiederer, U. Schmidt, D. Dubbers, and W. Kaiser, A long ballistic supermirror guide for cold neutrons at ILL, *Nucl. Instrum. Methods Phys. Res., Sect. A* **485**, 453 (2002).
- [37] H. Abele, D. Dubbers, H. H ase, M. Klein, A. Kn opfler, M. Kreuz, T. Lauer, B. M arkisch, D. Mund, V. Nesvizhevsky, A. Petoukhov, C. Schmidt, M. Schumann, and T. Soldner, Characterization of a ballistic supermirror neutron guide, *Nucl. Instrum. Methods Phys. Res., Sect. A* **562**, 407 (2006).
- [38] V. Wagner, H. Friedrich, and P. Wille, Performance of a high-tech neutron velocity selector, *Physica (Amsterdam)* **180B**, 938 (1992).
- [39] T. Soldner, A. Petoukhov, and C. Plonka, Installation and first tests of the new PF1b polariser, Report No. ILL03-SO10T, Institut Laue-Langevin, 2002.
- [40] M. Kreuz, V. Nesvizhevsky, A. Petoukhov, and T. Soldner, The crossed geometry of two super mirror polarizers—a new method for neutron beam polarization and polarization analysis, *Nucl. Instrum. Methods Phys. Res., Sect. A* **547**, 583 (2005).
- [41] T. Soldner *et al.*, Towards polarisation analysis with 10^{-4} accuracy, Report No. 3-07-235, Institut Laue-Langevin, 2011.

- [42] C. Klauser, J. Chastagnier, D. Jullien, A. Petoukhov, and T. Soldner, High precision depolarisation measurements with an opaque test bench, *J. Phys. Conf. Ser.* **340**, 012011 (2012).
- [43] C. Klauser, T. Bigault, N. Rebrova, and T. Soldner, Ultra-sensitive depolarization study of polarizing CoTi supermirrors with the opaque test bench, *Phys. Procedia* **42**, 99 (2013).
- [44] C. Klauser, T. Bigault, P. Böni, P. Courtois, A. Devishvili, N. Rebrova, M. Schneider, and T. Soldner, Depolarization in polarizing supermirrors, *Nucl. Instrum. Methods Phys. Res., Sect. A* **840**, 181 (2016).
- [45] D. Dubbers, H. Abele, S. Baeßler, B. Märkisch, M. Schumann, T. Soldner, and O. Zimmer, A clean, bright, and versatile source of neutron decay products, *Nucl. Instrum. Methods Phys. Res., Sect. A* **596**, 238 (2008).
- [46] C. Roick, D. Dubbers, B. Märkisch, H. Saul, and U. Schmidt, Electron time-of-flight: A new tool in β -decay spectroscopy, *Phys. Rev. C* **97**, 035502 (2018).
- [47] D. Dubbers, Magnetic guidance of charged particles, *Phys. Lett. B* **748**, 306 (2015).
- [48] S. Agostinelli *et al.* (GEANT4 Collaboration), GEANT4—a simulation toolkit, *Nucl. Instrum. Methods Phys. Res., Sect. A* **506**, 250 (2003).
- [49] K. Lefmann and K. Nielsen, McStas, a general software package for neutron ray-tracing simulations, *Neutron News* **10**, 20 (1999).
- [50] P. Willendrup, E. Farhi, and K. Lefmann, McStas 1.7 - a new version of the flexible Monte Carlo neutron scattering package, *Physica (Amsterdam)* **350B**, E735 (2004).
- [51] C. Raven, Erste Messungen mit Perkeo II: β -Asymmetrie im Neutron-Zerfall, Diploma thesis, Universität Heidelberg, 1995.
- [52] D. H. Wilkinson, Analysis of neutron β -decay, *Nucl. Phys.* **A377**, 474 (1982).
- [53] R. T. Shann, Electromagnetic effects in the decay of polarized neutrons, *Nuovo Cimento A* **5**, 591 (1971).
- [54] F. Glück and K. Tóth, Order- α radiative corrections for semileptonic decays of polarized baryons, *Phys. Rev. D* **46**, 2090 (1992).
- [55] A. N. Ivanov, M. Pitschmann, and N. I. Troitskaya, Neutron β^- decay as a laboratory for testing the standard model, *Phys. Rev. D* **88**, 073002 (2013).
- [56] D. Dubbers, H. Saul, B. Märkisch, T. Soldner, and H. Abele, Exotic decay channels are not the cause of the neutron lifetime anomaly, *Phys. Lett. B* **791**, 6 (2019).
- [57] N. Cabibbo, Unitary Symmetry and Leptonic Decays, *Phys. Rev. Lett.* **10**, 531 (1963).
- [58] M. Kobayashi and T. Maskawa, CP -violation in the renormalizable theory of weak interaction, *Prog. Theor. Phys.* **49**, 652 (1973).
- [59] A. P. Serebrov, E. A. Kolomensky, A. K. Fomin, I. A. Krasnoshchekova, A. V. Vassiljev, D. M. Prudnikov, I. V. Shoka, A. V. Chechkin, M. E. Chaikovskiy, V. E. Varlamov, S. N. Ivanov, A. N. Pirozhkov, P. Geltenbort, O. Zimmer, T. Jenke, M. Van der Grinten, and M. Tucker, Neutron lifetime measurements with a large gravitational trap for ultracold neutrons, *Phys. Rev. C* **97**, 055503 (2018).
- [60] R. W. Pattie *et al.*, Measurement of the neutron lifetime using a magneto-gravitational trap and in situ detection, *Science* **360**, 627 (2018).
- [61] V. F. Ezhov, A. Z. Andreev, G. Ban, B. A. Bazarov, P. Geltenbort, A. G. Glushkov, V. A. Knyazkov, N. A. Kovrizhnykh, G. B. Krygin, O. Naviliat-Cuncic, and V. L. Ryabov, Measurement of the neutron lifetime with ultracold neutrons stored in a magneto-gravitational trap, *Pis'ma Zh. Eksp. Teor. Fiz.* **107**, 707 (2018) [*JETP Lett.* **107**, 671 (2018)].
- [62] A. Czarnecki, W. J. Marciano, and A. Sirlin, Neutron Lifetime and Axial Coupling Connection, *Phys. Rev. Lett.* **120**, 202002 (2018).
- [63] W. J. Marciano and A. Sirlin, Improved Calculation of Electroweak Radiative Corrections and the Value of V_{ud} , *Phys. Rev. Lett.* **96**, 032002 (2006).
- [64] R. W. Pattie, K. P. Hickerson, and A. R. Young, Limits on tensor coupling from neutron β decay, *Phys. Rev. C* **88**, 048501 (2013).
- [65] R. W. Pattie, K. P. Hickerson, and A. R. Young, Erratum: Limits on tensor coupling from neutron β decay, *Phys. Rev. C* **92**, 069902(E) (2015).